Sandwich-like $MnO_x/Ni_{1-x}Mn_xO_y$@nanoporous nickel/MnO_x architecture with high areal/volumetric capacitance

Hua-Jun Qiu *, Xiao Li, Hai-Tao Xu, Yu Wang *

The State Key Laboratory of Mechanical Transmissions and School of Chemistry and Chemical Engineering, Chongqing University, Chongqing 400044, China

ARTICLE INFO

ABSTRACT

Hierarchical sandwich-like $MnO_x/Ni_{1-x}Mn_xO_y$@nanoporous nickel/MnO_x nano-architecture was fabricated by dealloying a $Ni_{25}Mn_{75}$ precursor in 1.0 M $(NH_4)_2SO_4$ solution followed by electrochemical oxidation in 1.0 M KOH solution. The dealloying process would generate both uniform nanoporous structure (chemical dealloying) and nanoporous structure with big crack channels (electrochemical dealloying at high potentials) with similar ligament-pore size of less than 10 nm. The electrochemical oxidation process then generates Ni/Mn mixed oxides/hydroxides filled in the nanopores by oxidizing the highly active nanoscale NiMn alloy ligaments. At the same time, the dissolved Mn ions in the nanopores (produced during the dealloying process) will be oxidized to form Mn oxides/hydroxides nanosheets attached to the nanoporous Ni surface when they diffuse out of the nanopores. With the highly conductive NiMn ligament core and large amount of metal oxides/hydroxides formed both in the nanopores and on the out-surface, the sandwich-like nanocomposite exhibits a high areal capacitance ($\sim$7 F cm^{-2}) with excellent rate performance and cycling stability when used as a free-standing supercapacitor electrode.

© 2015 Published by Elsevier Ltd.

1. Introduction

Due to the high power density and long lifespan, electrochemical supercapacitors are considered to be one of the most promising energy storage devices [1,2]. Compared with nanostructured carbon materials, recently, transition metal oxides (e.g., MnO_2, Co_3O_4, NiO, etc.) have attracted much research interest due to their low cost, environmental friendliness, and high theoretical capacitance from surface reversible redox reactions [2–10]. However, the poor electrical and ionic conductivities greatly limit their capacitor performance, especially at high rates [2]. To solve this problem, recently, the growth of nanostructured metal oxides on conductive free-standing substrates has developed. This design makes the auxiliary components like conductive additives and binders completely unnecessary. As a result, the fabricated binder-free electrodes exhibit high mass specific capacitances when only the mass of deposited metal oxides is counted [11–17]. However, their areal/volumetric capacitance is still very low due to the large pore size of most used conducting substrates. For example, the widely used commercial Ni foam and graphene/graphite foam (obtained by using Ni foam as a template [11,14,18]) possesses pore sizes of several hundred micrometers [19–22].

From the application standpoint, enhancing the utilization rate of the limited volume in a portable electronic device is very important. Effects have been made by multi-step deposition of metal oxides on conductive substrates such as Ni foam or physical compression of active metal oxides (or graphene) to improve the utilization rate of volume [15,16,23]. It is well-known that a proper electrode material with both a large specific surface area for high activity and a 3D interconnected nano-network for high conductivity would greatly enhance the specific capacitance and rate performance. In this contribution, to achieve a high areal/volumetric capacitance, we fabricated a free-standing and highly conductive nanoporous Ni (np-Ni) electrode by chemically etching a single-phase $Ni_{25}Mn_{75}$ alloy sheet. The nanopore space was then filled with Ni/Mn mixed oxides/hydroxides by electrochemical oxidation of the highly active NiMn alloy nano-ligaments in 1.0 M KOH solution. Interestingly, the dissolved Mn ion (if not removed by complete dealloying and washing) can be simultaneously deposited on the np-Ni surface forming a sandwich-like $MnO_x/Ni_{1-x}Mn_xO_y$@np-Ni/MnO_x nano-architecture (illustrated in Scheme 1). Owing to the high electronic conductivity from the Ni core nano-network, the efficient utilization of nanopore space and the contribution from surface MnO_x nanosheets, the nanoporous

* Corresponding authors.
  E-mail addresses: hjqiu@cqu.edu.cn (H.-J. Qiu), wangy@cqu.edu.cn (Y. Wang).
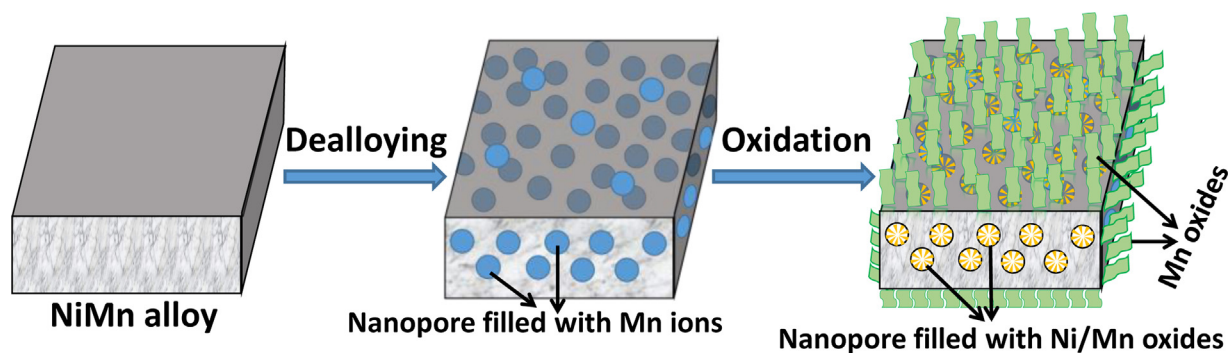
Scheme 1. Schematic illustration of the fabrication process of the sandwich-like architecture.

composite exhibits a high areal/volumetric capacitance compared with most reported results.

2. Experimental

Ni$_{25}$Mn$_{75}$ alloy ingot was prepared by melting pure Ni and Mn (>99.9 at.%) in an arc melting furnace filled with Ar. The ingot was then annealed at 900 °C for 1 day for the homogenization and followed by cold-rolling to an alloy sheet with a thickness of 95–100 μm at room temperature. Nanoporous Ni was prepared by chemically or electrochemcially dealloying Ni$_{25}$Mn$_{75}$ alloy sheet in 1.0 M (NH$_4$)$_2$SO$_4$ aqueous solutions. The just-dealloyed-through sample ($\sim$3.5 h dealloying and still bubbling in the dealloying solution), without washing, was transferred to 1 M KOH aqueous solution and electrochemically oxidized by continuous cyclic voltammetry (CV) cycling from -0.2 to 0.6 V vs. saturated calomel electrode (SCE) for 300 cycles to obtain the MnO$_x$/Ni$_{1-x}$Mn$_x$O$_y$@np-Ni/MnO$_x$ composite which was used as a binder-free super-capacitor electrode directly in the same solution. The changes of the CV curves during the electrochemical oxidation process were shown in Fig. S1 (Supporting Information). In comparison, a completely dealloyed np-Ni ($\sim$7 h dealloying and bubbling stopped) which was washed thoroughly with pure water has also been studied for comparison.

The samples were characterized by X-ray diffraction (XRD, Bruker D8 Advance X-ray diffractometer using a Cu Ka radiation at a scan rate of 0.04° s^{-1}) and X-ray photoelectron spectroscopy (XPS, ESCALab250 analyzer with Al Ka). The microstructures were characterized by transmission electron microscopy (TEM at 200 kV, JEOL JEM-2100F) and scanning electron microscopy (SEM at 5 kV, JEOL JSM-7800F) equipped with an energy-dispersive X-ray spectrometer (EDS). Electrochemical experiments were carried out on an electrochemical workstation (CHI 660e) in a three-electrode cell with a Pt foil as counter electrode and a SCE as reference electrode. The area of the samples immersed into the electrolyte was controlled to be $\sim$0.2 cm^{-2}. The areal specific capacitance (C) was calculated by the formula: $C = I\Delta t / S\Delta V$, where I is the current, Δt is the discharge time, ΔV is the voltage range and S is the nominal area of the free-standing electrode.

3. Results and discussion

3.1. Chemical dealloying and the electrochemical performance

Fig. 1a shows the plane-view low magnification SEM image of the sandwich-like np-Ni-based nano-architecture. It is observed that with a short dealloying time and dissolved Mn ion, after electrochemical oxidation, thin nanosheet-like MnO$_x$ structures with a thickness of several hundred nanometers are uniformly formed on the np-Ni surface forming a sandwich-like architecture

(inset in Fig. 1a). A zoom-in SEM image of the broken section shows that the middle part possesses uniform nanoporous structure with ligament-pore size of less than 10 nm (Fig. 1b). While for completely (long-time) dealloyed sample without the Mn ion residue, the surface of the sample (np-Ni) is very clean with all the grains connected to each other (inset in Fig. 1c). It should be noted that with longer dealloying time and more Mn removed, the completely dealloyed sample should have more void space inside, however, SEM image (Fig. 1c) shows that it possesses a quite similar ligament/pore size. The phenomenon of np-Ni is quite different from that of dealloyed nanoporous Au whose ligament/pore size coarsens quickly with dealloying time. The relatively stable and finer structure of np-Ni should be due to the very low surface diffusion rate of Ni compared with that of Au at room temperature [24].

The microstructure of middle np-Ni was further characterized by TEM and high-resolution TEM. As shown in Fig. 1d, clear contrast of the bright pores and dark ligaments are uniformly distributed, confirming the nanoporous structure. Due to the formation of Ni/Mn oxides/hydroxides on the ligament surface by electrochemical oxidation, the ligament is very rough and the nanopore size is obviously smaller than the ligament size. Some formed thin Ni/Mn oxides/hydroxides crystals within the pores are indicated by arrows (Fig. 1e). Probably due to the poor crystallization at room temperature and very small crystal size, XRD pattern of the sandwich-like architecture exhibited no obvious diffraction peaks. To make the dealloyed sample better crystallized, we then dealloyed one sample at an elevated temperature of 50 °C. XRD pattern of this sample exhibits obvious face-centered cubic (fcc) structure with three main peaks located at 43.5°, 50.7° and 75.1°, respectively (Fig. 1f). Compared with that of the precursor, the three diffraction peaks shift to high angles, indicating the decrease of the lattice constant by the removal of Mn which has a bigger atomic size. The diffraction peaks also become much broader due to the formed nanoscale metallic ligaments. Besides these three peaks, an additional broader peak located between 60° and 65° can be assigned to the formed Ni/Mn oxide.

EDS analysis from the surface shows that the Mn content is $\sim$60 at.% due to the formed Mn oxides (Fig. 2a). While from the section part, EDS result shows the Mn is $\sim$36 at.% (Fig. 2b), confirming the sandwich-like structure. For the long-time completely dealloyed sample, EDS analysis from both surface and section exhibits a similar Mn content ($\sim$23 at.%, Fig. 2c). To further demonstrate the formed sandwich-like architecture, the surface sensitive XPS analysis was carried out. The surface is mainly comprised of Mn and O, confirming the surface Mn oxides/hydroxides structure. As shown in Fig. 3a, the Mn 2p3/2 shows a main peak at binding energy of 641.9 eV, indicating that MnO$_2$ or MnOOH are likely the dominant species [25]. Other species such as Mn^{2+} may also exist considering the broad feature of the peak.